



A smart hydrogel for on-demand delivery of antibiotics and efficient eradication of biofilms

Jingjing Hu¹, Chenglin Zhang², Lei Zhou², Qianyu Hu¹, Yanlong Kong³, Dianwen Song^{2*}, Yiyun Cheng^{1*} and Yadong Zhang^{3,4*}

ABSTRACT Biofilm-associated infections are difficult to treat in the clinics because the bacteria embedded in biofilm are ten to thousand times more resistant to traditional antibiotics than planktonic ones. Here, a smart hydrogel comprised of aminoglycoside antibiotics, pectinase, and oxidized dextran was developed to treat local biofilm-associated infections. The primary amines on aminoglycosides and pectinase were reacted with aldehyde groups on oxidized dextran *via* a pH-sensitive Schiff base linkage to form the hydrogel. Upon bacterial infection, the increased acidity triggers the release of both pectinase and aminoglycoside antibiotics. The released pectinase efficiently degrades extracellular polysaccharides surrounding the bacteria in biofilm, and thus greatly sensitizes the bacteria to aminoglycosides. The smart hydrogel efficiently eradicated biofilms and killed the embedded bacteria both *in vitro* and *in vivo*. This study provides a promising strategy for the treatment of biofilm-associated infections.

Keywords: biofilm, smart hydrogels, antibacterial, enzyme, antibiotics

INTRODUCTION

Biofilm is an aggregate of bacteria surrounded by a high density of biomacromolecules such as polysaccharides, proteins and extracellular nucleic acids. The dense matrix in biofilm blocks the penetration of antibiotics to attack the bacteria, and facilitates the embedded bacteria to escape from immune systems [1,2]. In addition, the hypoxic environment in biofilm inactivates most antibiotics on the bacteria [3]. It is reported that bacteria embedded in biofilm are ten to thousand times more resistant to antibacterial drugs than planktonic ones, and biofilm has

been considered as one of the major causes for bacteria resistance [4–8]. The persistent bacteria in biofilm survived after antibiotic treatment are responsible for infection recurrence. Furthermore, biofilm formed on implantable medical devices may cause implant failure and difficult-to-treat chronic infections, leading to increased medical cost and mortality [9,10]. Therefore, it is highly desirable to develop novel strategies to eradicate the biofilm and kill the encased bacteria [11–16].

Nanomedicines and biomaterials have shown great promise in the treatment of various diseases in recent years [17–20]. To treat biofilm-associated infections, quorum sensing inhibitors [21,22], nanoparticles [23–25], antimicrobial peptides [26], antisense nucleic acids [27,28], enzyme mimetics [29], polymers [30–32] and antifouling coatings [33–36] with the activity of inhibiting biofilm formation were developed in the past decade. These compounds or materials could sensitize biofilm infections to conventional antibiotics [6,37]. In addition, photosensitizers and plasmonic nanoparticles were used in combination with lasers to eradicate the biofilm *via* photodynamic and photothermal therapy [38–43]. Extracellular polysaccharides are the major component of biofilm matrix [44]. The polysaccharides, such as alginate, Pel and Psl, stick bacteria and biofilm matrix together like a glue, and protect the bacteria from immune systems. The polysaccharides produced by different bacteria are complicated, and the strain-to-strain variability in polysaccharide components is significant [45]. We could use natural enzymes that can degrade the complex polysaccharides and thus convert the biofilm-encased bacteria to planktonic ones. Pectinases (Pec) are a group of en-

¹ Shanghai Key Laboratory of Regulatory Biology, School of Life Sciences, East China Normal University, Shanghai 200241, China

² Department of Orthopedics, Shanghai General Hospital, School of Medicine, Shanghai Jiao Tong University, Shanghai 200080, China

³ Department of Orthopaedics, Fengxian Hospital Affiliated to Anhui University of Science and Technology, Shanghai 201499, China

⁴ Department of Orthopaedics, Fengxian Hospital Affiliated to Southern Medical University, Shanghai 201499, China

* Corresponding authors (emails: dianwen.song@shgh.cn (Song D); yycheng@mail.ustc.edu.cn (Cheng Y); zhangyadong6@126.com (Zhang Y))

zymes that can degrade the complex polysaccharides in plant cell wall into oligosaccharides [46]. These enzymes were widely used in food industry, such as fruit softening, fruit juice lucidification, and coffee and tea fermentations. Pec immobilized on membranes can be used as anti-biofilm coating in the treatment of waste water [47,48]. A previous study reported that a fungal strain *Aspergillus clavatus* MTCC1323 can degrade the biofilms of *Pseudomonas aeruginosa* (*P. aeruginosa*) and *Bacillus subtilis* (*B. subtilis*) by produced enzymes such as Pec, protease, and amylase [49]. Based on these studies, the natural enzyme Pec has high clinical translation potential to break down polysaccharides in biofilm and sensitize the bacteria to conventional antibiotics such as aminoglycosides.

Most biofilm infections occur during surgery, and therefore local therapeutic formulations such as antibiotic-loaded hydrogels, cements, and beads were used in clinics [9]. Hydrogels have attracted great interest in this field due to sustained drug release, excellent tissue adhesion and biocompatibility [50–56]. In this study, we proposed a hydrogel consisted of Pec, aminoglycosides and oxidized dextran to treat biofilm-associated infections (Fig. 1a). Aminoglycosides possess multiple amine groups that can react with aldehyde groups on oxidized dextran to form hydrogels *via* pH-sensitive Schiff base bond [57]. The aminoglycoside antibiotics could be released in an on-demand manner upon bacterial infection, and the hydrogels could be fully degraded once the cross-linked aminoglycosides were released. Like aminoglycosides, Pec have a large number of primary amine groups on the surface, which makes it possible to prepare a responsive Pec hydrogel with oxidized polysaccharides such as dextran [58]. The hydrogel containing both Pec and aminoglycosides were expected to break down the mature biofilm by released Pec and kill the bacteria inside *via* released aminoglycoside antibiotics (Fig. 1b). We hope to provide a facile and efficient hydrogel formulation for the treatment of biofilm-associated infections.

EXPERIMENTAL SECTION

Materials

Dextran (450–650 kDa) was purchased from Sigma-Aldrich (St. Louis, USA). Aminoglycosides including amikacin (Ami), netilmicin, isepamicin, gentamicin, tobramycin, and neomycin were purchased from Dalian Meilun Biotech. (Dalian, China). Pec (500 U mg⁻¹), agar, and 3-(4,5-dimethylthiazol-2-yl)-2,5-diphenyltetrazolium bromide (MTT) were purchased from Sangon Biotech.

(Shanghai, China). Tryptone, yeast extract, tryptic soy broth (TSB) and mueller-hinton broth (MH) were purchased from Oxoid (Basingstoke, UK). Live-dead BacLight™ Bacterial Viability Kit (L13152) was purchased from Thermo Fisher Scientific. 3-Mercaptopropionic acid, *o*-phthalaldehyde, boric acid and crystal violet were obtained from Aladdin (Shanghai, China). *P. aeruginosa* (PAO1) and *Staphylococcus aureus* (*S. aureus*, USA300) were obtained from ATCC.

Preparation and characterization of the hydrogels

Briefly, the dextran was oxidized using the method established in our previous study [57], and the oxidation degree was detected to be 52%. Then, 100 μ L complex hydrogel was prepared by mixing 60 μ L oxidized dextran (60 mg mL⁻¹), 5 μ L Ami (30 mg mL⁻¹) and 35 μ L Pec (600 mg mL⁻¹) solutions together; the gel was formed within a few minutes at pH 9 for Ami/Pec solution. Rheological properties of the hydrogel were investigated by using a rheometer (TA Instrument, USA). For the thixotropic property measurement, the hydrogel was broken and recovered by alternating the oscillation force between 100% and 1% strains for three cycles, and the modulus was recorded at a constant angular frequency of 10 rad s⁻¹. For the shear thinning study, the viscosity was measured with a shear rate swept from 0.01 to 80 s⁻¹ at a constant strain of 1%, and the hydrogel was also injected through a syringe (1.2 mm×30 mm, the outer diameter is 1.2 mm and the length of the needle is 30 mm) to confirm the shear thinning property. For Ami hydrogel, 100 μ L gel was prepared by mixing 60 μ L oxidized dextran (60 mg mL⁻¹), 5 μ L Ami (30 mg mL⁻¹), and 35 μ L deionized water together, and for Pec hydrogel, 100 μ L gel was prepared by mixing 60 μ L oxidized dextran (60 mg mL⁻¹), 35 μ L Pec (600 mg mL⁻¹), and 5 μ L deionized water together.

In vitro drug release from the hydrogels

Complex hydrogels (500 μ L) were prepared as described above and the gels were immersed in 10 mL phosphate buffered saline (PBS) at pH 7.4 and 5.0, respectively. Two milliliter of the solutions was collected at determined time intervals, followed by replenishment with 2 mL fresh buffer. The concentration of released Ami in the collected samples was evaluated by a well-established *o*-phthalaldehyde derivatization method [59]. The calibration curve was $y = 0.6006x + 0.13$ ($R^2 = 0.9976$), where x is the Ami concentration (mg mL⁻¹), and y is the absorbance of samples at 333 nm. The concentration of released Pec in the collected samples was determined according to the

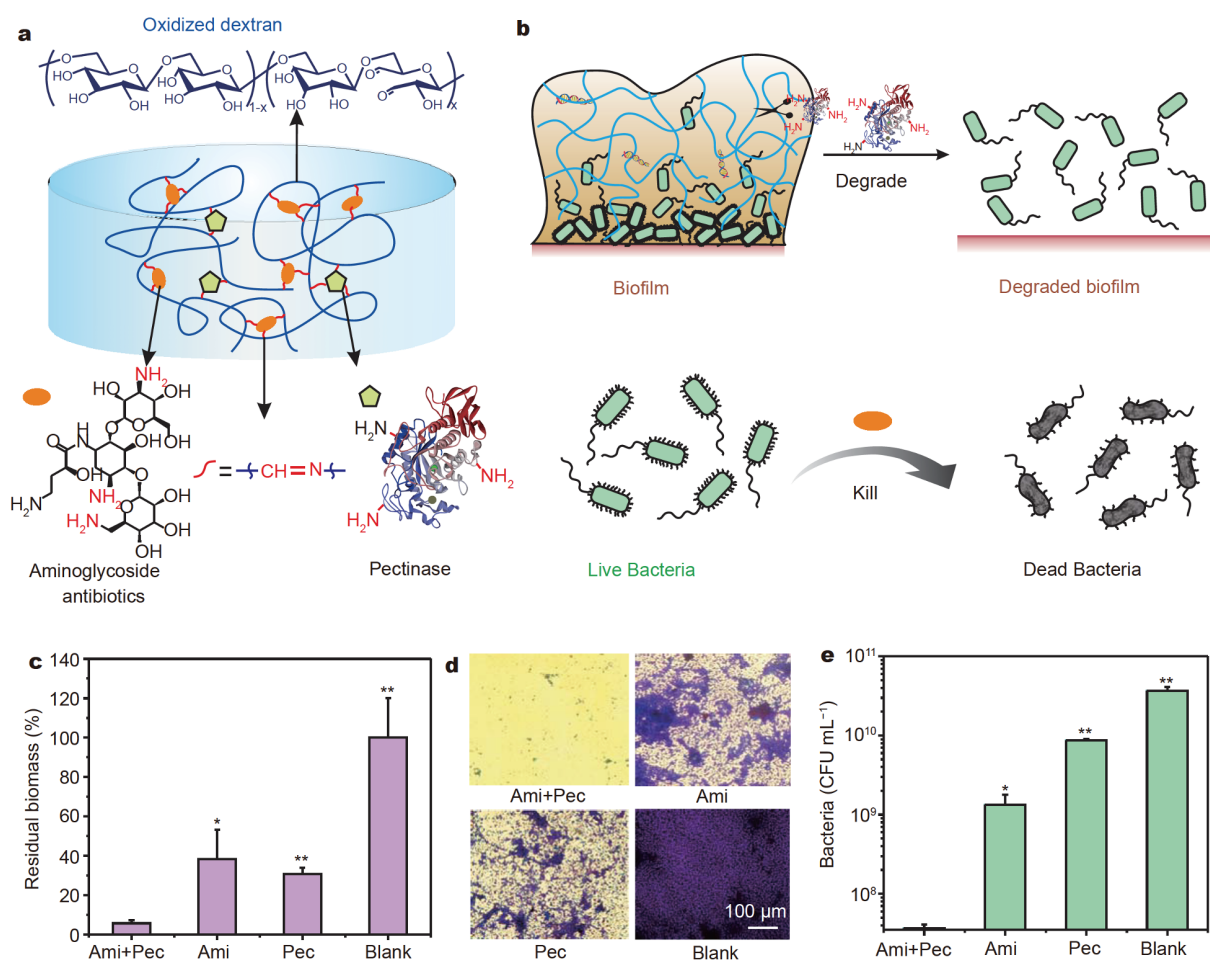


Figure 1 A smart hydrogel for the treatment of biofilm-associated infections. (a) Preparation of the hydrogel by mixing oxidized dextran, aminoglycosides and Pec together via the formation of Schiff base linkages. (b) Illustration of the biofilm eradication and bacteria killing by Pec and Ami released from the hydrogel. (c) Residual biomass generated by *P. aeruginosa* biofilm on a glass coverslip after treatment with Ami (16 μg mL⁻¹), Pec (20 mg mL⁻¹), and Ami/Pec mixture (16 μg mL⁻¹ for Ami, and 20 mg mL⁻¹ for Pec), respectively. (d) Crystal violet staining of the coverslips in (c). (e) Counts of live *P. aeruginosa* in the treated *P. aeruginosa* biofilms in (c). **P* < 0.05, ***P* < 0.01 analyzed by student's *t*-test.

solution absorbance at 280 nm. The calibration curve was $y = 0.4009x - 0.0093$ ($R^2 = 0.9997$), where x is the Pec concentration (mg mL⁻¹), and y is the absorbance of samples at 280 nm. Three repeats were conducted for each sample.

MIC assay

P. aeruginosa colonies were isolated from the Luria-Bertani (LB) plate and re-suspended in 5 mL sterile LB medium. For planktonic bacteria, the bacteria suspensions (OD₆₀₀ (optical density at 600 nm) of 0.5) were adjusted to 10⁶ CFU mL⁻¹ using MH medium, and 90 μL diluted suspensions were added into the wells of a 48-well plate. Ten microliter of antibiotic solutions was prepared with MH medium using a two-fold serial dilution method

and added into each well (the final antibiotic concentrations were ranged from 0.125 to 128 μg mL⁻¹ for aminoglycosides, 0.5 to 512 μg mL⁻¹ for amoxicillin, tetracycline and ciprofloxacin, 0.1 to 102.4 μg mL⁻¹ for polymyxin E, respectively). For *P. aeruginosa* biofilm, the bacteria suspensions were cultured in the wells for 48 h to obtain mature biofilm. On the third day, the bacteria suspensions were removed and the wells were washed with PBS to remove the floating bacteria. After that, 100 μL antibiotic solutions were prepared using MH medium and diluted using a 2-fold dilution method as described above. The antibiotic concentrations were ranged from 1 to 1024 μg mL⁻¹ for aminoglycosides and polymyxin E, and 5 to 5120 μg mL⁻¹ for amoxicillin, tetracycline and ciprofloxacin. After incubation for 24 h, the lowest con-

centration at which the bacteria solution turned clear and transparent was recognized as the minimum inhibition concentration (MIC) value. Pec and mixture of Pec and antibiotics of different concentrations were tested as described above. For Pec only, the final concentrations of Pec in the medium were ranged from $62.5 \mu\text{g mL}^{-1}$ to 64 mg mL^{-1} , while for the Pec/Ami mixture, the Pec concentration was kept constant at 20 mg mL^{-1} , and the Ami concentration was varied from 0.125 to $128 \mu\text{g mL}^{-1}$. The MIC values of antibiotics or Pec/antibiotic mixture on *S. aureus* were tested by a similar procedure. *S. aureus* colonies were isolated from the tryptic soy agar (TSA) plate, and the colonies were resuspended in sterile TSB for activation. Three repeats were conducted for each sample.

In vitro biofilm inhibition and antibacterial assay

Ami was chosen as the model aminoglycoside in the following studies. To evaluate the biofilm inhibition ability of Pec, the *P. aeruginosa* suspensions (10^6 CFU mL^{-1}) were seeded in 48-well plates, and Ami/Pec mixture solutions were added into the bacteria suspensions at final concentrations of $0.5 \mu\text{g mL}^{-1}$ and 20 mg mL^{-1} for Ami and Pec, respectively. After incubation for 24 h, the suspensions were removed and the remaining bacteria on the plate were carefully rinsed with PBS for three times to remove the planktonic bacteria. The remaining biofilm in the wells was quantified using a standard crystal violet assay. Generally, the wells were dried and added with $150 \mu\text{L}$ methanol, then incubated for 15 min to immobilize the biofilm. The methanol was removed and the biofilm was naturally dried for 30 min. An aliquot of 1 wt% crystal violet solution ($150 \mu\text{L}$) was added into the wells to stain the biofilm for 10 min. Then, the crystal violet solutions were removed and the wells were washed thoroughly with distilled water and dried before photographed. To quantitatively measure the amount of biofilm, the stained biofilms were dissolved with $200 \mu\text{L}$ 33% (v/v) acetic acid, and the absorbance of yielding solution at 590 nm was measured by a microplate reader (Multiskan Go, ThermoFisher). Free Ami and free Pec were tested as controls.

To evaluate the ability of Pec to eradicate mature biofilm, $300 \mu\text{L}$ fresh bacteria suspensions (10^6 CFU mL^{-1}) was cultured in a 48-well plate. The bacteria suspensions were removed and the wells were supplemented with fresh LB medium every 24 h. The mature biofilms were obtained after 48 h. Then, Ami/Pec mixture ($16 \mu\text{g mL}^{-1}$ for Ami, $5\text{--}40 \text{ mg mL}^{-1}$ for Pec) in LB medium was added into the wells and further incubated for 24 h. The sus-

pensions were removed and the wells were carefully rinsed with PBS for three times. The residual biofilm was quantitatively measured as mentioned above. Free Ami and free Pec were tested as controls. The effect of incubation time on biofilm eradication was also investigated. Mature biofilms were established as described above, and the concentration of Pec was fixed at 20 mg mL^{-1} . All the procedures were the same except for the incubation times were set at 3, 6, 9, 12, 20, and 24 h, respectively. After incubation, the amount of biomass in the wells was tested as described above.

The biofilm inhibition activity of Pec, Ami and Pec/Ami hydrogels on *P. aeruginosa* and *S. aureus* was tested as follows. Generally, bacteria suspensions (10^6 CFU mL^{-1}) were cultured in 48-well plate for 48 h to allow the formation of mature biofilm. The biofilm in the wells was then treated with $40 \mu\text{L}$ hydrogel and further added with $300 \mu\text{L}$ fresh medium, and cultured for another 24 h. The biomass in the treated biofilm was measured as described above. The number of viable bacteria in the treated biofilm was measured by the plate colony counting method. Three repeats were conducted for each sample.

Mature *P. aeruginosa* biofilms were also formed on glass coverslips. Generally, sterile glass coverslips ($2.0 \text{ cm} \times 2.0 \text{ cm}$) were placed in a 6-well plate, and then seeded with 1.5 mL *P. aeruginosa* suspensions (10^6 CFU mL^{-1}) and incubated for 48 h to obtain mature biofilm-covered coverslips. The bacteria suspensions were removed and the coverslips were rinsed with sterilized PBS for three times. After that, 1.5 mL Ami ($16 \mu\text{g mL}^{-1}$), Pec (20 mg mL^{-1}) and Pec/Ami (20 mg mL^{-1} Pec and $16 \mu\text{g mL}^{-1}$ Ami) solutions in LB media were added into the wells containing glass coverslips, and incubated for another 24 h. Then the biofilm on the coverslips were stained with crystal violet solution as described above. The residual biofilms were also detached from the glass coverslips and re-suspended in PBS. The number of live bacteria in the biofilm after treatment was measured using the plate colony counting method. In addition, the treated biofilm on each coverslip was also stained using a Live-dead Baclight™ bacterial viability kit ($200 \mu\text{L}$, $6 \mu\text{mol L}^{-1}$ SYTO 9 and $30 \mu\text{mol L}^{-1}$ propidium iodide) and incubated for 10 min in dark to observe live and dead bacteria after treatment. The stained coverslips were imaged using a fluorescent microscopy (Olympus IX71, Japan). For confocal studies, 1.5 mL *P. aeruginosa* suspensions (10^6 CFU mL^{-1}) were added into confocal dishes, the medium was replaced every 24 h and the bacteria were cultured for 48 h to allow biofilm forma-

tion. After that, 200 μL hydrogels were added into the wells, followed by replenishment with 1.5 mL fresh medium and incubation with the biofilm for 24 h, the media were removed and the biofilm was washed with PBS buffer. Finally, the bacteria in biofilm were stained by the Live/dead BacLight™ bacterial viability kit, and the solutions were removed before observation by confocal laser scanning microscopy (CLSM, Leica SP5, Germany).

Inhibition zone assay

P. aeruginosa and *S. aureus* collected from the biofilm were respectively diluted with LB and TSB at a final concentration of 10^6 CFU mL^{-1} , then poured into a dish. After freezing, three holes with a diameter around 0.8 cm were made on the culture media, and the holes were added with 25 μL Ami hydrogel, Pec hydrogel, Ami/Pec complex hydrogel, respectively. The hydrogels were prepared as described above. After incubation overnight, the dishes were photographed for observation.

Scanning electron microscopy (SEM) characterization

Mature *P. aeruginosa* biofilm was formed on circular coverslips with a diameter of 2.0 cm in a 6-well plate as described above, and then 200 μL Ami hydrogel, Pec hydrogel, and Ami/Pec complex hydrogel were added into the wells, and further supplemented with 1.5 mL fresh LB medium. After incubation for 24 h, the residual biofilm on the glass coverslip was immobilized and dehydrated, and finally sputter-coated with platinum for SEM imaging (S-4800, Hitachi, Japan). Untreated biofilm was tested as a control.

Biocompatibility assay

The toxicity of the prepared hydrogels on NIH 3T3 cells was evaluated by an MTT assay. Cells were cultured in Dulbecco's modified Eagle's medium (DMEM, Gibco) supplemented with 1% streptomycin/penicillin and 10% heat-inactivated fetal bovine serum (FBS, Gemini) in humidified 5% CO_2 at 37°C, and seeded in 96-well plates at a density of 10^4 cells per well. Complex hydrogel (200 μL) was prepared as described above and immersed in 2 mL DMEM without FBS at 37°C for 24 h, and the gel extract solutions were collected as the medium for cell culture after supplemented with 10% FBS. The cell viability was measured by a standard MTT method. Five repeats were conducted for each sample. For hemolysis assay, red blood cells (RBCs) were separated from whole blood by using the method described previously [60], and 200 μL RBCs were dispersed in 9.8 mL PBS to obtain 2% RBC suspension. Then, 20 μL complex hydrogel was in-

cubated with 1 mL RBC suspension at 37°C for 1 h. Triton X-100 (0.5 wt%) and PBS were tested as positive and negative controls, respectively. After incubation, the mixtures were centrifuged at 2000 r min^{-1} for 5 min, and the supernatants were collected. The absorption of solutions at 540 nm (A) was measured using a microplate reader (Thermo, USA). The hemolysis percentage was calculated as $(A_{\text{Sample}} - A_{\text{PBS}}) / (A_{\text{Triton X-100}} - A_{\text{PBS}}) \times 100$.

In vivo biofilm eradication assay

Six-week-old Kunming (KM) mice were employed to test the anti-biofilm activity of complex hydrogels *in vivo*. All the animal experiments in this study were approved by the Ethics Committee for Animal Experimentation in East China Normal University (ECNU). Twenty mice were randomly divided into four groups, with five mice in each group. A medical silicon foley catheter ($d = 2.7$ mm) was cut into 8 mm length and incubated in *P. aeruginosa* suspensions (10^6 CFU mL^{-1}) for two days to allow biofilm formation on the catheters. The catheters were subcutaneously implanted into the back of mice and the wound were sewn up. Then, 100 μL Ami/Pec complex hydrogel, Ami hydrogel, and Pec hydrogel were injected at the implanted catheters. After 6 days, the mice were sacrificed and the catheters in the mice were harvested. The biofilm on the catheters were stained by crystal violet, and the numbers of live bacteria on the catheters were counted by plate colony counting method as described above.

In vivo antibacterial effect against P. aeruginosa biofilm

Six-week-old KM mice were employed for *in vivo* antibacterial assay. *P. aeruginosa* was cultured for 48 h to form mature biofilms as described above, and the collected biofilms were re-suspended in fresh LB medium to OD_{600} value of 0.1 (10^8 CFU mL^{-1}). The mice were divided into four groups with five mice in each group. The mice were subcutaneously injected with 100 μL PBS, Ami/Pec complex hydrogel, Ami hydrogel, and Pec hydrogel, respectively. After 30 min, 70 μL *P. aeruginosa* biofilm solutions (10^8 CFU mL^{-1}) were injected into the hydrogel sites. The survival and body weight of mice during the treatment were monitored. After 3 days, the animals were sacrificed, and the infected skin tissues, and the main organs including heart, liver, spleen, lung and kidney were collected. The lung and liver were photographed before homogenization. The tissues were then homogenized with 1 mL PBS, and the numbers of bacteria in the tissues were measured by the plate colony counting method as described above. For the infected

skin tissues, the paraffin sectioned tissues were analyzed by Gram-staining and photographed by an optical microscope (Olympus IX71, Japan).

RESULTS AND DISCUSSION

It is reported that bacteria in biofilm are much more resistant to antibiotics than planktonic ones [61]. We firstly tested the MIC values of several commonly used antibiotics on planktonic bacteria and biofilm, respectively. The results demonstrated that the MIC values of these antibiotics on *P. aeruginosa* biofilm were 20–1280 times higher than those for planktonic bacteria (Fig. S1). In this study, we proposed the use of Pec to degrade the polysaccharides in biofilm, and thus sensitize biofilm infections to antibiotics. Aminoglycoside antibiotics at sub-inhibitory concentrations may induce biofilm formation, and accelerate drug resistance on *P. aeruginosa* [8]. The MIC of Ami on planktonic *P. aeruginosa* is $2 \mu\text{g mL}^{-1}$, and thus we used Ami at a concentration of 0.25 MIC to confirm the biofilm inhibitory effect of Pec. As shown in Fig. S2, the combination of Ami and Pec efficiently inhibited the generated biomass by planktonic *P. aeruginosa*, and the presence of Pec enhanced the antibacterial activity of Ami at the sub-inhibitory concentration. We further tested the effect of Pec on the degradation of mature biofilm. Pec could also break down the mature biofilm by *P. aeruginosa*, and the biofilm dispersal efficiency is dependent on Pec concentration and incubation time (Fig. S3a and b). The combination of Ami and Pec efficiently inhibited the biomass of mature *P. aeruginosa* biofilm to 5.8%, while free Pec and free Ami treatments showed much more residual biomass (Fig. 1c). The efficient biofilm dispersal by Ami and Pec is further confirmed by crystal violet staining. The biofilm treated with Ami and Pec mixture showed minimal crystal violet staining (Fig. 1d). The MIC value of Ami on *P. aeruginosa* biofilm is $512 \mu\text{g mL}^{-1}$; however, the value for Ami and Pec mixture is decreased by 16-fold compared with that of free Ami (Fig. S4). Considering that Pec cannot inhibit *P. aeruginosa* at the highest concentration in this study (64 mg mL^{-1}), we concluded that Pec efficiently break down the biofilm and sensitize the bacteria to Ami. We also counted the number of live *P. aeruginosa* in the biofilm after treatment. The number of live bacteria was decreased by at least three orders of magnitude when incubated with the Ami and Pec mixture (Fig. 1e), and the efficient killing of *P. aeruginosa* in biofilm is confirmed by live-dead bacteria staining (Fig. S5). Similar results were obtained on *S. aureus* (Figs S4 and S6).

We further prepared the Ami/Pec complex hydrogel by

mixing Ami, Pec and oxidized dextran solutions together. Aminoglycosides are excellent gelators due to high density of amine groups on the oligosaccharide scaffold, which ensures both high aqueous solubility and reactivity to form crosslinking networks [62–64]. The amine groups on both Ami and Pec are capable of forming dynamic connections with aldehyde groups on oxidized dextran *via* Schiff base linkage [57]. Ami hydrogel and Pec hydrogel were prepared as control materials. The concentrations of Ami, Pec and oxidized dextran in the control gels were equal to those in the complex gel. Transparent and stable hydrogels were formed within several minutes for all the three hydrogels (Fig. 2a). The Ami/Pec complex hydrogel exhibited an excellent thixotropic property (Fig. 2b). Besides, the gel showed a shear-thinning property and could be injected by a syringe (Fig. 2c). These rheological properties allow the prepared hydrogel to be administrated *via* local injection. It showed a pH-responsive drug release behavior due to the Schiff base linkage between Ami/Pec and oxidized dextran. The release of Ami and Pec from the complex gel was generally simultaneous. Both Ami and Pec showed sustained release behavior at pH 7.4, and the release of both drugs was accelerated at pH 5.0 (Fig. 2d). It has been verified that the growth of bacterial biofilm may induce an acidic microenvironment (Fig. S7), allowing a pH-responsive release of the antibiotics and enzymes. Since all the components in the gel including Pec, Ami and oxidized dextran are non-toxic, the complex hydrogel showed minimal toxicity on NIH3T3 cells (Fig. 2e), and no hemolysis reaction (Fig. 2f).

The biofilm eradication and antibacterial activity of the Ami/Pec complex hydrogel were further investigated. The *P. aeruginosa* biofilms on glass coverslips treated with Ami/Pec complex gel, Ami gel and Pec gel, respectively were characterized by SEM. As shown in Fig. 3a, bacteria aggregates were surrounded by silk-like fibers for untreated *P. aeruginosa* biofilms. The fibers were significantly decreased when the biofilm was treated with Pec gels; however, lots of *P. aeruginosa* were remained on the coverslip after treatment due to low antibacterial activity of the enzyme. In comparison, Ami gel treatment efficiently decreased the number of *P. aeruginosa*, but bacteria aggregates with silk-like fibers were still observed on the glass. The complex gel efficiently eradicated the biofilm and killed the bacteria. The *P. aeruginosa* biofilm was cultured in confocal dishes and further treated with the hydrogels. The live and dead *P. aeruginosa* in the biofilm after treatment were stained using a Live-dead BacLight™ bacterial viability kit and observed by a con-

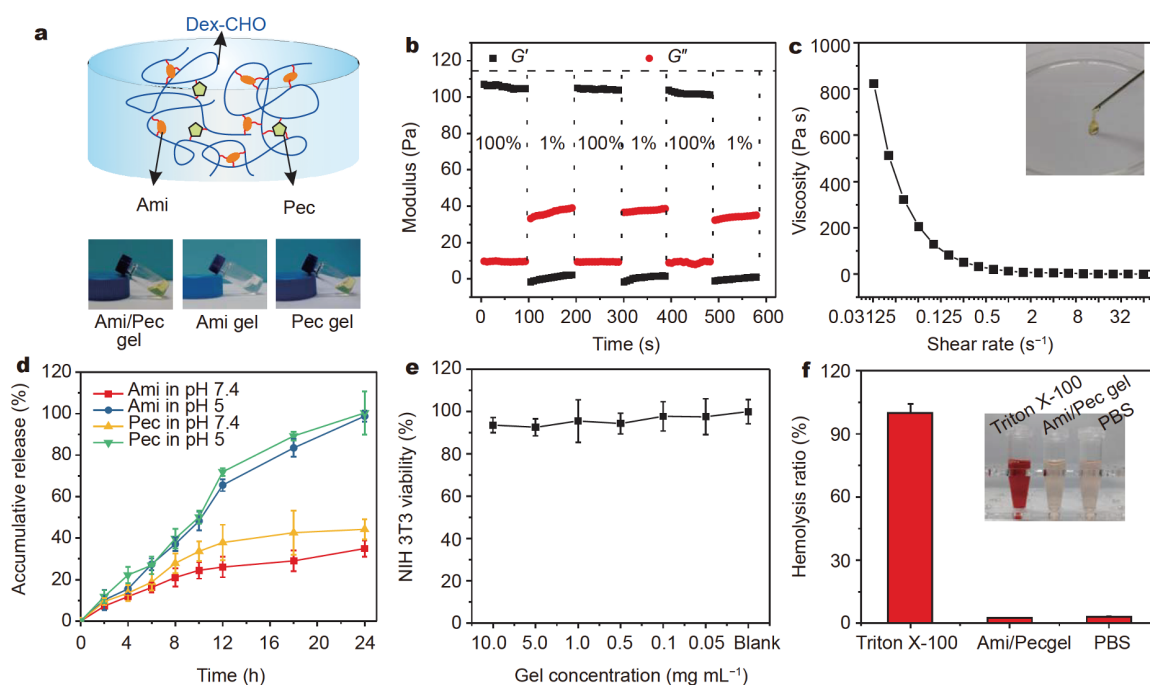


Figure 2 Properties of the Ami/Pec complex hydrogel. (a) Preparation of the Ami/Pec complex hydrogel. Ami gel and Pec gel with equal concentrations of oxidized dextran and Ami/Pec were prepared as controls. (b) Thixotropic property of the complex hydrogel, the angular frequency was kept constant at 10 rad s^{-1} with an alternative strain of 1% and 100%. (c) Shear thinning property of the complex hydrogel. The inserted image is the injection of complex gel through a syringe ($1.2 \text{ mm} \times 30 \text{ mm}$). (d) Accumulative release of Ami and Pec from the Ami/Pec complex hydrogel at pH 7.4 and 5.0, respectively. (e) Viability of NIH 3T3 cells treated with the complex hydrogel at different concentrations of the complex hydrogel. Triton X-100 and PBS were tested as the positive and negative controls, respectively.

focal microscope. As shown in Fig. 3b, nearly all the *P. aeruginosa* in biofilm were observed with red fluorescence when treated with Ami/Pec complex hydrogel, while lots of live bacteria stained with green fluorescence were observed in all the control groups. These results clearly demonstrated high biofilm dispersal activity of the complex hydrogel. After treatment with the Ami/Pec complex hydrogel, the biomass of the mature biofilm decreased to 9% (Fig. 3c) and the number of live *P. aeruginosa* decreased by two orders of magnitude (Fig. 3d). In comparison, the Ami gel failed to efficiently break down the mature biofilm and showed a less pronounced antibacterial effect against the *P. aeruginosa* biofilm. Inhibition zone assay also confirmed the sensitized antibacterial activity of Ami/Pec complex hydrogel on the *P. aeruginosa* and *S. aureus* biofilms in comparison with the Ami gel and the Pec gel (Fig. 3e and Fig. S8).

The formation of bacterial biofilm on implants, catheters, and endotracheal tubes is the leading cause of medical device-related infections in the clinics. We therefore examined the biofilm eradication ability of the complex hydrogel *in vivo*. Mature *P. aeruginosa* biofilms

were formed on silicon foley catheters (diameter 2.7 mm, length 8 mm), and the catheters were subcutaneously implanted at the back of mice (Fig. 4a). The hydrogels were injected at the catheter site, and the infection experiments were lasted for six days. The harvested catheters were stained by crystal violet and the numbers of live *P. aeruginosa* on the catheters were counted. As shown in Fig. 4b, violet films were observed on the catheters treated with PBS, Ami gel and Pec gel, while the biofilms were greatly inhibited on the catheter treated with Ami/Pec complex gel. In addition, the remaining live *P. aeruginosa* on the catheter after complex gel treatment decreased significantly (Fig. 4c), which was three orders of magnitude lower than those on PBS-treated catheters, and two orders of magnitude lower than those treated with Ami gel and Pec gel. These results suggest that the Ami/Pec complex hydrogel efficiently break down the *P. aeruginosa* biofilms *in vivo* and the released Pec from complex gel sensitize *P. aeruginosa* biofilm to Ami.

We finally investigated the *in vivo* antibacterial activity of Ami/Pec complex hydrogel on *P. aeruginosa* biofilm-associated infections. The hydrogels were subcutaneously

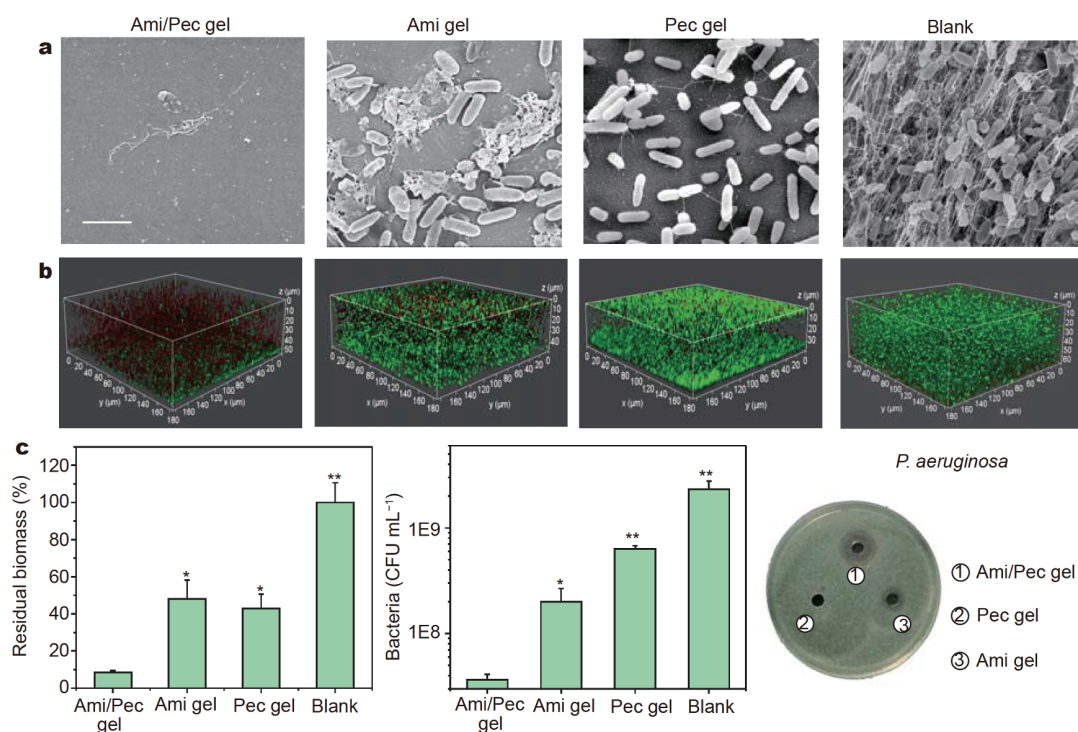


Figure 3 *In vitro* biofilm eradication and antibacterial activity of the complex hydrogel. (a) SEM images of the *P. aeruginosa* biofilm formed on a glass coverslip. Scale bar: 2 μm . (b) Confocal images of the treated *P. aeruginosa* biofilm by a live-dead bacteria staining. (c) Residual biomass and (d) the count of live bacteria in the biofilm after treatment. (e) Inhibition zone of the hydrogels on *P. aeruginosa* biofilm. * $P < 0.05$, ** $P < 0.01$ analyzed by student's *t*-test.

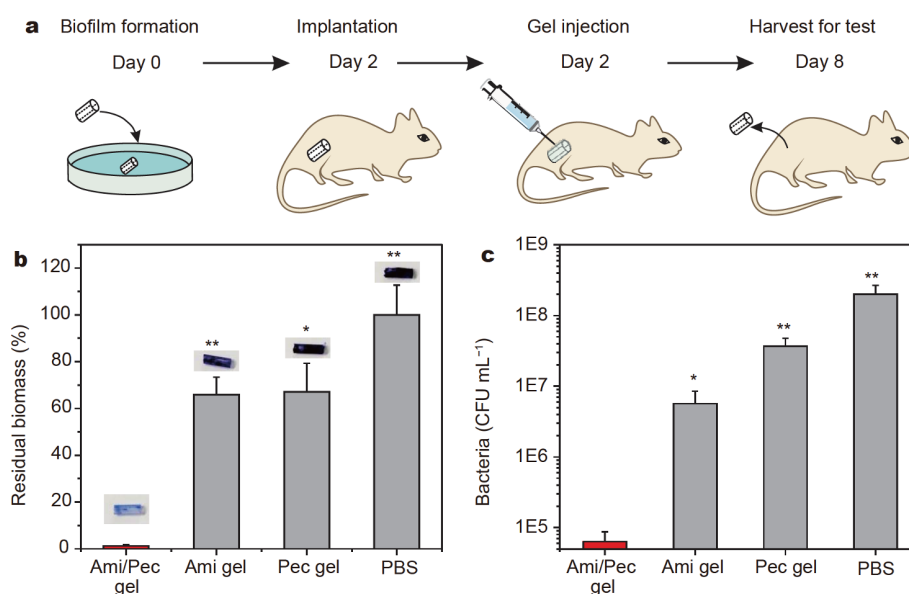


Figure 4 *In vivo* biofilm eradication and antibacterial activity of the complex hydrogel. (a) Illustration of catheter implantation model. (b) Residual biomass on the catheter after treatment. The inserted images on bars are the photographs of the harvested catheters stained by crystal violet. (c) Counts of live *P. aeruginosa* on the catheters after treatment. * $P < 0.05$, ** $P < 0.01$ analyzed by student's *t*-test.

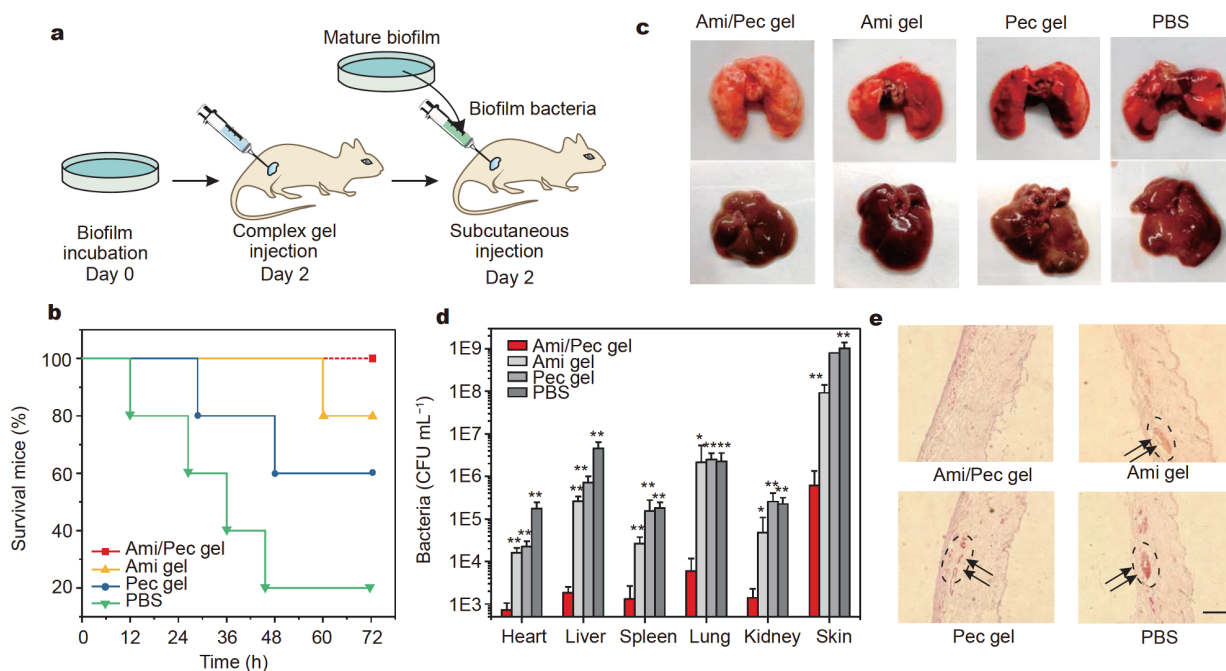


Figure 5 Performance of the hydrogel in the treatment of biofilm infections *in vivo*. (a) Illustration of biofilm infection model. (b) Survival curve of the mice during the treatment. (c) Photographs of lung and liver harvested from the treated mice. (d) Counts of live bacteria in the organs harvested from the treated mice. (e) Gram staining of the skin harvested from the infection site after treatment. The arrows indicate stained *P. aeruginosa* in the skin tissue sections. Scale bar: 200 μm . $P < 0.05$, $**P < 0.01$ analyzed by student's *t*-test.

injected to the back of mice, and the mice were then infected with *P. aeruginosa* biofilm at the gel site (Fig. 5a). The survival rate of mice decreased to 20% for the PBS group after 3-day treatment, and the numbers for the Pec gel and the Ami gel groups were 60% and 80%, respectively. In comparison, all the animals were survival for the complex gel group (Fig. 5b). The collected lung and liver from the complex gel group are observed in normal appearance, while significant ecchymosis and bleeding points were found on the tissues from the control groups (Fig. 5c). This result is consistent with the bacteria counting results shown in Fig. 5d. The *P. aeruginosa* numbers in the organs collected from complex gel treated mice were significantly lower than those in the control groups. Besides, Gram staining of the skin tissues collected from infected site showed that a limited number of bacteria were observed on the tissue sections from the complex gel group (Fig. 5e), while obvious bacterial infections were observed in the tissues of control groups. These results together confirmed the potent *in vivo* anti-biofilm and antibacterial activity of the Ami/Pec complex hydrogel.

CONCLUSIONS

In this study, we designed a smart hydrogel consisting of

Ami, Pec and oxidized dextran for on-demand delivery of Pec for biofilm eradication and aminoglycoside antibiotics for killing bacteria. Pec in the gel efficiently broke down the mature biofilm generated by bacteria such as *P. aeruginosa*, and sensitized the biofilm-encased bacteria to antibiotics. The complex hydrogel efficiently eradicated biofilm infection both *in vitro* and *in vivo*, and represents a promising formulation for local treatment of biofilm-associated infections.

Received 26 May 2020; accepted 7 August 2020;
published online 26 October 2020

- 1 Flemming HC, Wingender J, Szewzyk U, *et al.* Biofilms: An emergent form of bacterial life. *Nat Rev Microbiol*, 2016, 14: 563–575
- 2 Rybtke M, Hultqvist LD, Givskov M, *et al.* Pseudomonas aeruginosa biofilm infections: Community structure, antimicrobial tolerance and immune response. *J Mol Biol*, 2015, 427: 3628–3645
- 3 de Beer D, Stoodley P, Roe F, *et al.* Effects of biofilm structures on oxygen distribution and mass transport. *Biotechnol Bioeng*, 1994, 43: 1131–1138
- 4 Liu R, Chen X, Falk SP, *et al.* Nylon-3 polymers active against drug-resistant *Candida albicans* biofilms. *J Am Chem Soc*, 2015, 137: 2183–2186
- 5 Xi Y, Wang Y, Gao J, *et al.* Dual corona vesicles with intrinsic antibacterial and enhanced antibiotic delivery capabilities for effective treatment of biofilm-induced periodontitis. *ACS Nano*,

- 2019, 13: 13645–13657
- 6 Liu Y, Shi L, Su L, *et al.* Nanotechnology-based antimicrobials and delivery systems for biofilm-infection control. *Chem Soc Rev*, 2019, 48: 428–446
 - 7 Su L, Li Y, Liu Y, *et al.* Recent advances and future prospects on adaptive biomaterials for antimicrobial applications. *Macromol Biosci*, 2019, 19: 1900289
 - 8 Hoffman LR, D'Argenio DA, Maccoss MJ, *et al.* Aminoglycoside antibiotics induce bacterial biofilm formation. *Nature*, 2005, 436: 1171–1175
 - 9 Ashbaugh AG, Jiang X, Zheng J, *et al.* Polymeric nanofiber coating with tunable combinatorial antibiotic delivery prevents biofilm-associated infection *in vivo*. *Proc Natl Acad Sci USA*, 2016, 113: E6919–E6928
 - 10 Walther R, Nielsen SM, Christiansen R, *et al.* Combatting implant-associated biofilms through localized drug synthesis. *J Control Release*, 2018, 287: 94–102
 - 11 Ding X, Wang A, Tong W, *et al.* Biodegradable antibacterial polymeric nanosystems: A new hope to cope with multidrug-resistant bacteria. *Small*, 2019, 15: 1900999
 - 12 Ding X, Duan S, Ding X, *et al.* Versatile antibacterial materials: An emerging arsenal for combatting bacterial pathogens. *Adv Funct Mater*, 2018, 28: 1802140
 - 13 Pelgrift RY, Friedman AJ. Nanotechnology as a therapeutic tool to combat microbial resistance. *Adv Drug Deliver Rev*, 2013, 65: 1803–1815
 - 14 Liu Y, Busscher HJ, Zhao B, *et al.* Surface-adaptive, antimicrobially loaded, micellar nanocarriers with enhanced penetration and killing efficiency in *Staphylococcal* biofilms. *ACS Nano*, 2016, 10: 4779–4789
 - 15 Chen X, Zhang X, Lin F, *et al.* One-step synthesis of epoxy group-terminated organosilica nanodots: A versatile nanoplatform for imaging and eliminating multidrug-resistant bacteria and their biofilms. *Small*, 2019, 15: 1901647
 - 16 Ran HH, Cheng X, Bao YW, *et al.* Multifunctional quaternized carbon dots with enhanced biofilm penetration and eradication efficiencies. *J Mater Chem B*, 2019, 7: 5104–5114
 - 17 Lv J, Fan Q, Wang H, *et al.* Polymers for cytosolic protein delivery. *Biomaterials*, 2019, 218: 119358
 - 18 Zhou Z, Yan Y, Wang L, *et al.* Melanin-like nanoparticles decorated with an autophagy-inducing peptide for efficient targeted photothermal therapy. *Biomaterials*, 2019, 203: 63–72
 - 19 Shen W, Wang R, Fan Q, *et al.* Natural polyphenol inspired polycatechols for efficient siRNA delivery. *CCS Chem*, 2020, 2: 146–157
 - 20 Ren L, Lv J, Wang H, *et al.* A coordinative dendrimer achieves excellent efficiency in cytosolic protein and peptide delivery. *Angew Chem Int Ed*, 2020, 59: 4711–4719
 - 21 Cutrona N, Gillard K, Ulrich R, *et al.* From antihistamine to anti-infective: Loratadine inhibition of regulatory PASTA kinases in staphylococci reduces biofilm formation and potentiates β -lactam antibiotics and vancomycin in resistant strains of *Staphylococcus aureus*. *ACS Infect Dis*, 2019, 5: 1397–1410
 - 22 Shaaban M, Elgaml A, Habib ESE. Biotechnological applications of quorum sensing inhibition as novel therapeutic strategies for multidrug resistant pathogens. *Microbial Pathogenesis*, 2019, 127: 138–143
 - 23 Duan F, Feng X, Jin Y, *et al.* Metal-carbenicillin framework-based nanoantibiotics with enhanced penetration and highly efficient inhibition of MRSA. *Biomaterials*, 2017, 144: 155–165
 - 24 Huma Z, Javed I, Zhang Z, *et al.* Nanosilver mitigates biofilm formation *via* FapC amyloidosis inhibition. *Small*, 2020, 16: 1906674
 - 25 Xie Y, Liu Y, Yang J, *et al.* Gold nanoclusters for targeting methicillin-resistant *Staphylococcus aureus in vivo*. *Angew Chem Int Ed*, 2018, 57: 3958–3962
 - 26 Mwangi J, Yin Y, Wang G, *et al.* The antimicrobial peptide ZY4 combats multidrug-resistant *Pseudomonas aeruginosa* and *Acinetobacter baumannii* infection. *Proc Natl Acad Sci USA*, 2019, 116: 26516–26522
 - 27 Narenji H, Teymournejad O, Rezaee MA, *et al.* Antisense peptide nucleic acids against *ftsZ* and *efaA* genes inhibit growth and biofilm formation of *Enterococcus faecalis*. *Microbial Pathogenesis*, 2019, 139: 103907
 - 28 Bordeau V, Felden B. Curli synthesis and biofilm formation in enteric bacteria are controlled by a dynamic small RNA module made up of a pseudoknot assisted by an RNA chaperone. *Nucleic Acids Res*, 2014, 42: 4682–4696
 - 29 Chen Z, Wang Z, Ren J, *et al.* Enzyme mimicry for combating bacteria and biofilms. *Acc Chem Res*, 2018, 51: 789–799
 - 30 Wang M, Shi J, Mao H, *et al.* Fluorescent imidazolium-type poly (ionic liquid)s for bacterial imaging and biofilm inhibition. *Biomacromolecules*, 2019, 20: 3161–3170
 - 31 Mauro N, Schillaci D, Varvarà P, *et al.* Branched high molecular weight glycopolypeptide with broad-spectrum antimicrobial activity for the treatment of biofilm related infections. *ACS Appl Mater Interfaces*, 2018, 10: 318–331
 - 32 Tan H, Peng Z, Li Q, *et al.* The use of quaternised chitosan-loaded PMMA to inhibit biofilm formation and downregulate the virulence-associated gene expression of antibiotic-resistant staphylococcus. *Biomaterials*, 2012, 33: 365–377
 - 33 Zeng Q, Zhu Y, Yu B, *et al.* Antimicrobial and antifouling polymeric agents for surface functionalization of medical implants. *Biomacromolecules*, 2018, 19: 2805–2811
 - 34 Gao Q, Feng T, Huang D, *et al.* Antibacterial and hydroxyapatite-forming coating for biomedical implants based on polypeptide-functionalized titania nanospikes. *Biomater Sci*, 2020, 8: 278–289
 - 35 Zhang L, Cole JM. Anchoring groups for dye-sensitized solar cells. *ACS Appl Mater Interfaces*, 2015, 7: 3427–3455
 - 36 Hwang G, Koltisko B, Jin X, *et al.* Nonleachable imidazolium-incorporated composite for disruption of bacterial clustering, exopolysaccharide-matrix assembly, and enhanced biofilm removal. *ACS Appl Mater Interfaces*, 2017, 9: 38270–38280
 - 37 Siala W, Kuchariková S, Braem A, *et al.* The antifungal caspofungin increases fluorquinolone activity against *Staphylococcus aureus* biofilms by inhibiting *N*-acetylglucosamine transferase. *Nat Commun*, 2016, 7: 13286
 - 38 de Miguel I, Prieto I, Albornoz A, *et al.* Plasmon-based biofilm inhibition on surgical implants. *Nano Lett*, 2019, 19: 2524–2529
 - 39 Zhao Y, Guo Q, Dai X, *et al.* A biomimetic non-antibiotic approach to eradicate drug-resistant infections. *Adv Mater*, 2019, 31: 1806024
 - 40 Deng Q, Sun P, Zhang L, *et al.* Porphyrin MOF dots-based, function-adaptive nanoplatform for enhanced penetration and photodynamic eradication of bacterial biofilms. *Adv Funct Mater*, 2019, 29: 1903018
 - 41 Hu D, Li H, Wang B, *et al.* Surface-adaptive gold nanoparticles with effective adherence and enhanced photothermal ablation of methicillin-resistant *Staphylococcus aureus* biofilm. *ACS Nano*, 2017, 11: 9330–9339

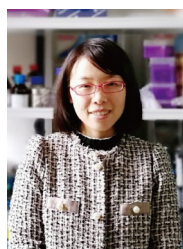
- 42 Dai X, Zhao Y, Yu Y, *et al.* All-in-one NIR-activated nanoplat-forms for enhanced bacterial biofilm eradication. *Nanoscale*, 2018, 10: 18520–18530
- 43 Jia Q, Song Q, Li P, *et al.* Rejuvenated photodynamic therapy for bacterial infections. *Adv Healthcare Mater*, 2019, 8: 1900608
- 44 Jennings LK, Storek KM, Ledvina HE, *et al.* Pel is a cationic exo-polysaccharide that cross-links extracellular DNA in the *Pseudo-monas aeruginosa* biofilm matrix. *Proc Natl Acad Sci USA*, 2015, 112: 11353–11358
- 45 Colvin KM, Irie Y, Tart CS, *et al.* The Pel and Psl polysaccharides provide *Pseudomonas aeruginosa* structural redundancy within the biofilm matrix. *Environ Microbiol*, 2012, 14: 1913–1928
- 46 Kashyap DR, Vohra PK, Chopra S, *et al.* Applications of pectinases in the commercial sector: A review. *Bioresource Tech*, 2001, 77: 215–227
- 47 Villa F, Secundo F, Polo A, *et al.* Immobilized hydrolytic enzymes exhibit antibiofilm activity against *Escherichia coli* at sub-lethal concentrations. *Curr Microbiol*, 2015, 71: 106–114
- 48 Borszcz V, Boscato TP, Flach J, *et al.* Bacterial biofilm removal using solid-state-produced enzymes. *Industrial Biotech*, 2017, 13: 311–318
- 49 Singh V, Verma N, Banerjee B, *et al.* Enzymatic degradation of bacterial biofilms using *Aspergillus clavatus* MTCC 1323. *Micro-biology*, 2015, 84: 59–64
- 50 Li S, Dong S, Xu W, *et al.* Antibacterial hydrogels. *Adv Sci*, 2018, 5: 1700527
- 51 Wang X, Wang C, Wang X, *et al.* A polydopamine nanoparticle-knotted poly(ethylene glycol) hydrogel for on-demand drug deliv-ery and chemo-photothermal therapy. *Chem Mater*, 2017, 29: 1370–1376
- 52 Hu J, Chen Y, Li Y, *et al.* A thermo-degradable hydrogel with light-tunable degradation and drug release. *Biomaterials*, 2017, 112: 133–140
- 53 Wang C, Wang D, Dai T, *et al.* Skin pigmentation-inspired poly-dopamine sunscreens. *Adv Funct Mater*, 2018, 28: 1802127
- 54 Cheng X, Li M, Wang H, *et al.* All-small-molecule dynamic covalent gels with antibacterial activity by boronate-tannic acid gelation. *Chin Chem Lett*, 2020, 31: 869–874
- 55 Hu J, Wang H, Hu Q, *et al.* G-quadruplex-based antiviral hydro-gels by direct gelation of clinical drugs. *Mater Chem Front*, 2019, 3: 1323–1327
- 56 Wang J, Chen G, Zhao Z, *et al.* Responsive graphene oxide hy-drogel microcarriers for controllable cell capture and release. *Sci China Mater*, 2018, 61: 1314–1324
- 57 Hu J, Quan Y, Lai Y, *et al.* A smart aminoglycoside hydrogel with tunable gel degradation, on-demand drug release, and high anti-bacterial activity. *J Control Release*, 2017, 247: 145–152
- 58 Liu Z, Guo K, Zhao N, *et al.* Polysaccharides-based nanohybrids: promising candidates for biomedical materials. *Sci China Mater*, 2019, 62: 1831–1836
- 59 Hu J, Zheng Z, Liu C, *et al.* A pH-responsive hydrogel with potent antibacterial activity against both aerobic and anaerobic pathogens. *Biomater Sci*, 2019, 7: 581–584
- 60 Dai T, Wang C, Wang Y, *et al.* A nanocomposite hydrogel with potent and broad-spectrum antibacterial activity. *ACS Appl Mater Interfaces*, 2018, 10: 15163–15173
- 61 de Breij A, Riool M, Cordfunke RA, *et al.* The antimicrobial peptide SAAP-148 combats drug-resistant bacteria and biofilms. *Sci Transl Med*, 2018, 10: eaan4044
- 62 Li M, Wang H, Hu J, *et al.* Smart hydrogels with antibacterial properties built from all natural building blocks. *Chem Mater*, 2019, 31: 7678–7685
- 63 Hu J, Hu Q, He X, *et al.* Stimuli-responsive hydrogels with anti-bacterial activity assembled from guanosine, aminoglycoside, and a bifunctional anchor. *Adv Healthcare Mater*, 2020, 9: 1901329
- 64 Wang H, Cheng Y. All-small-molecule dynamic covalent hydrogels with multistimuli responsiveness. *Mater Chem Front*, 2019, 3: 472–475

Acknowledgements This work was supported by the National Key R&D Program of China, Synthetic Biology Research (2019YFA0904500), the National Natural Science Foundation of China (21725402 and 51672191), and the Natural Science Foundation of Shanghai (19ZR1415600). The authors acknowledge the ECNU Multifunctional Platform for Innovation (011) for the animal experiments.

Author contributions Hu J prepared and evaluated the *in vitro* antibacterial properties of the hydrogels; Hu J, Zhang C, Zhou L and Kong Y performed the *in vivo* experiments; Hu Q contributed to the physicochemical characterization of the hydrogel; Song D, Zhang Y and Cheng Y designed and supervised the study and wrote the manuscript. All the authors contributed to the general discussion.

Conflict of interest The authors declare that they have no conflict of interest.

Supplementary information Supporting data are available in the online version of the paper.



Jingjing Hu is an associate professor of biomaterials at the School of Life Science, East China Normal University. She received her PhD degree from the University of Science and Technology of China. Her research interests mainly focus on the design of antibacterial materials and smart hydrogels.



Dianwen Song is a full professor and chief physician at the Department of Orthopedics, Shanghai General Hospital, Shanghai Jiao Tong University. He received his MD and PhD degrees from the Second Military Medical University. His research interests focus on the development of tissue-engineered bone and mechanism of bone metastasis in malignancies.



Yiyun Cheng is a full professor of biomedical engineering at the School of Life Sciences, East China Normal University. He received his PhD degree from the University of Science and Technology of China and was a postdoctoral fellow at Washington University in St. Louis, MO. His research interests focus on the rational design of polymers for the delivery of biomacromolecules.



Yadong Zhang is a chief physician and professor at the Department of Orthopaedics, Fengxian Hospital affiliated to Southern Medical University. He received his PhD from Shanghai Jiao Tong University. He is expert in the treatment of spinal diseases. His research interests focus on the design of smart hydrogels and nanomedicines for bone repair and the treatment of bacterial infection.

可按需释放抗生素并高效清除生物被膜的智能水凝胶

胡婧婧¹, 张成林², 周磊², 胡倩瑜¹, 孔彦龙³, 宋滇文^{2*}, 程义云^{1*}, 张亚东^{3,4*}

摘要 生物被膜相关感染在临床上的治疗难度极大, 这是由于被包裹在被膜中的细菌对传统抗生素的抵抗力是浮游细菌的数十至数千倍. 本文研究开发了一种由氨基糖苷类抗生素、果胶酶以及氧化葡聚糖组成的智能水凝胶, 用于治疗与生物被膜相关的局部感染. 氨基糖苷和果胶酶结构中的伯胺可与氧化葡聚糖的醛基形成对pH敏感的希夫碱键, 从而形成凝胶. 当发生感染时, 局部增强的酸性会触发果胶酶和氨基糖苷类抗生素的释放, 所释放出的果胶酶可有效降解生物被膜中包裹在细菌周围的多糖, 从而提高细菌对氨基糖苷类药物的敏感度. 该智能水凝胶可有效清除生物膜, 并能在体内有效杀灭被膜中的细菌. 该研究为生物被膜相关感染的治疗提供了一种具有良好潜力的策略.